Compact system description for systems comprising a tilted plane parallel plate

Jack van den Eerenbeemd and Sjoerd Stallinga

A paraxial model describing the astigmatism generated by a plane-parallel plate is derived. This model fits the framework of the 4 × 4 matrix formalism that Arsenault used to describe cylindrical lenses. The framework including this new model is used to build a compact system description of a plane-parallel plate combined with a cylindrical lens, from which several imaging properties are derived. Calculation results are compared with ray-trace simulation results and measurements. Both the ray-trace and the experimental results are in excellent agreement with the calculated results.

OCIS codes: 080.2730, 220.4830, 210.4770.

1. Introduction

It is well known that like cylindrical lenses, a plane-parallel plate (PPP) in a diverging or converging beam generates astigmatism.[1] For cylindrical lenses Arsenault[2,3] proposed a 4 × 4 matrix formalism to describe the imaging properties of these lenses. In this paper we expand this matrix formalism with a paraxial model for the PPP. The formalism can now be used to describe systems comprising both PPPs and cylindrical lenses. To illustrate the usefulness of this we examine a servo branch of a DVD optical recording light path.

In optical recording devices the astigmatic focusing method is often used for controlling the distance between the lens and the disk.[4] The required astigmatism is often generated by a cylindrical lens or by a PPP in a converging beam. Normally the same detector used for generating the focus error is also used for generating a tracking signal by means of push–pull detection.[4] This means that ideally one of the focal lines of the astigmatic beam has to be oriented at 45° with respect to the push–pull lobes on the detector.

A cylindrical lens can always be rotated such that the astigmatism it generates fulfills the above-mentioned requirement. A PPP, however, is usually also used as a beam splitter. This means that the orientation of the astigmatism generated by a beam-splitting PPP depends on how the light path is oriented with respect to the tracks on an optical disk. For space reasons the light path might be oriented such that the astigmatism generated by a beam-splitting PPP is parallel to the push–pull lobes. This would require a sophisticated detector layout to generate both the focus-error and the tracking-error signals. Instead of a complicated detector a beam-splitting cube combined with a cylindrical lens can be used since a cube does not generate astigmatism in a converging beam. A beam-splitting cube, however, is bulkier compared with a beam-splitting PPP and generates spherical aberration in the light path toward the disk.

Here we present a novel solution where the astigmatism generated by the PPP is combined with that of a cylindrical lens such that the desired orientation and amount of astigmatism arises on the detector. A large number of parameters are involved in the design of such a system. This makes the use of a ray-tracing program to design the system rather awkward. We present in Section 2 a paraxial model for describing nonrotationally symmetric optical components that includes the description of the astigmatism generated by a PPP based on the 4 × 4 matrix formalism. Section 3 is used to present an example for which a system matrix is derived whose various general properties are discussed. In Section 4 the calculated results are compared to the numerical results obtained by ray tracing. The calculated results are then compared with measurements.

The authors are with Philips Research Laboratories, High Tech Campus 34, 5656 AE, Eindhoven, the Netherlands. J. van den Eerenbeemd's e-mail address is jack.van.den.eerenbeemd@philips.com.

Received 21 August 2006; accepted 8 September 2006; posted 20 September 2006 (Doc. ID 74179); published 4 January 2007.

0003-6935/07/030319-08$15.00/0

2. Theory

In this section first a general optical power matrix is derived that is used to describe toroidal, spherical, and cylindrical surfaces. Next the translation matrix is derived from which a representation of a PPP is obtained.

A. Derivation of the 4 × 4 Power Matrix

We start by considering the refraction of a narrow pencil of light concentrated around the chief ray that propagates in the direction $\mathbf{k}$, with $|\mathbf{k}| = 1$, by a surface (see Fig. 1). In a medium with refractive index n we then have

$$n\mathbf{k} = \left[\mu_x,\ \mu_y,\ \left(n^2 - \mu^2\right)^{1/2}\right], \tag{1}$$

where $\mu = (\mu_x^2 + \mu_y^2)^{1/2}$ is the absolute value of the projection of the propagation vector $n\mathbf{k}$ onto the XY plane. For an arbitrary ray inside the pencil the propagation direction is then given by $\mathbf{k} + \delta\mathbf{k}$, with $|\mathbf{k} + \delta\mathbf{k}| = 1$ and $|\delta\mathbf{k}| \ll 1$. From this we obtain

$$n(\mathbf{k} + \delta\mathbf{k}) = \left(\mu_x + \delta\mu_x,\ \mu_y + \delta\mu_y,\ \left(n^2 - (\boldsymbol{\mu} + \delta\boldsymbol{\mu})^2\right)\right)^{1/2}, \tag{2}$$

so,

$$n\delta\mathbf{k} = \left(\delta\mu_x,\ \delta\mu_y,\ \frac{-\boldsymbol{\mu}\cdot\delta\boldsymbol{\mu}}{\sqrt{n^2 - \mu^2}}\right). \tag{3}$$

Refraction occurs at a curved surface given by $z = f(x, y)$. For paraxial rays, f is approximated by expanding it in x and y to the second order:

$$z \approx \frac{1}{2}\sum_{ij} p_{ij} r_i r_j = \frac{1}{2}\left[p_{xx}x^2 + (p_{xy} + p_{yx})xy + p_{yy}y^2\right]. \tag{4}$$

An arbitrary ray intersects the surface close to the intersection point $\mathbf{r} = (x, y)$ of the chief ray. We will neglect the difference in the intersection points. The surface normal is defined as $\mathbf{a} = (a_x, a_y, [1 - a_x^2 - a_y^2)^{1/2}]$ with

$$-a_x = \frac{\partial z}{\partial x} = p_{xx}x + p_{xy}y,$$

$$-a_y = \frac{\partial z}{\partial y} = p_{yx}x + p_{yy}y. \tag{5}$$

Here p_{xy} was set equal to p_{yx}, which is valid because they act on the surface in the same indiscernible way. However, to keep the symmetry in the notation, they will both be used separately. Since $|a_x|, |a_y| \ll 1$, $\mathbf{a} \approx (a_x, a_y, 1)$. We can now formulate Snell's law as

$$n(\mathbf{k} + \delta\mathbf{k}) \times \mathbf{a} = n'(\mathbf{k}' + \delta\mathbf{k}') \times \mathbf{a}. \tag{6}$$

After expanding the cross product it is found that in the zeroth order $\mu_x = \mu_x'$ and $\mu_y = \mu_y'$ or $\mu = \mu'$. These are the chief ray invariants. In the first order we have

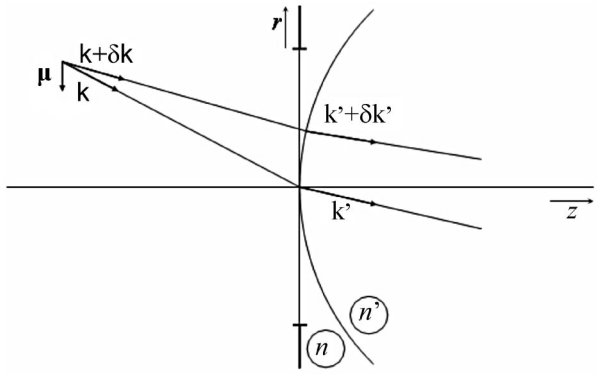

Fig. 1. Refraction of the chief ray and an arbitrary ray by a surface drawn in the meridional plane. The difference between the propagation vectors of both rays equals $\delta\mathbf{k}$.

$$\delta\mu_x - \sqrt{n^2 - \mu^2}a_x = \delta\mu_x' - \sqrt{n'^2 - \mu^2}a_x,$$

$$\delta\mu_y - \sqrt{n^2 - \mu^2}a_y = \delta\mu_y' - \sqrt{n'^2 - \mu^2}a_y. \tag{7}$$

And because at a single surface the position of a ray does not change $\mathbf{r} = \mathbf{r}'$, so we can write

$$\delta\boldsymbol{\mu}' = \delta\boldsymbol{\mu} - \left(\sqrt{n'^2 - \mu^2} - \sqrt{n^2 - \mu^2}\right) \times \begin{bmatrix} p_{xx} & p_{xy} \\ p_{yx} & p_{yy} \end{bmatrix}\mathbf{r} \equiv \delta\boldsymbol{\mu} + \mathbf{P}\mathbf{r}, \tag{8}$$

where $\mathbf{P}$ is the optical power matrix. Using partitioned matrices this reads

$$\begin{bmatrix} \mathbf{r}' \\ \delta\boldsymbol{\mu}' \end{bmatrix} = \begin{bmatrix} \mathbf{1} & \mathbf{0} \\ \mathbf{P} & \mathbf{1} \end{bmatrix}\begin{bmatrix} \mathbf{r} \\ \delta\boldsymbol{\mu} \end{bmatrix} = [\mathbf{L}]\begin{bmatrix} \mathbf{r} \\ \delta\boldsymbol{\mu} \end{bmatrix}, \tag{9}$$

where $\mathbf{1}$ is the 2×2 unit matrix, and $\mathbf{0}$ is a 2×2 null matrix.

To determine the power matrix of some simple surfaces we start by considering a part of the surface of a torus. The surface sag of a torus that is azimuthally symmetric about an axis in the XZ plane and parallel to the y axis with an inner radius R and a tube radius r is given by[5]

$$z = \pm(R \pm r) \pm \sqrt{\left(R \pm \sqrt{r^2 - y^2}\right)^2 - x^2}. \tag{10}$$

All the $\pm$signs in Eq. (10) are attributable to the four intersections of the torus with the z axis. Note that not all combinations give valid sags, i.e., $z = 0$ for $x, y = 0$. These $\pm$signs may be discarded by allowing negative values for R and r. By doing so and expanding Eq. (10) to the lowest orders in x and y we find

$$z \approx \frac{x^2}{2(R + r)} + \frac{y^2}{2r} + \mathrm{O}(x, y)^3 \quad R \neq -r. \tag{11}$$

By using Eq. (4) we define $1/R_x \equiv p_{xx} = 1/(R + r)$, $1/R_y \equiv p_{yy} = 1/r$, for the radii in the x and y direc-

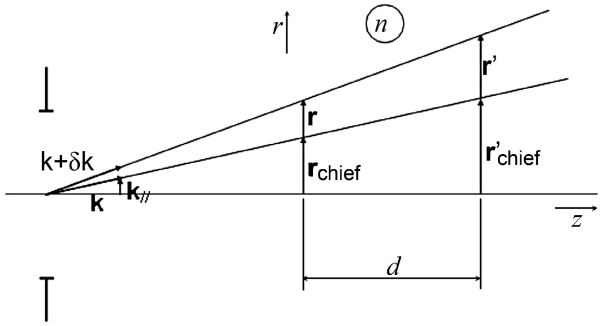

Fig. 2. Translation of the chief ray and an arbitrary ray over a distance d drawn in the meridional plane.

tions, and we have $p_{xy} = p_{yx} = 0$. Combining this with Eq. (8) we find for a paraxial object ($\mu \ll 1$) the power matrix for a toroidal surface,

$$\mathbf{P}_{\text{toroidal}} = -(n' - n)\begin{bmatrix} 1/R_x & 0 \\ 0 & 1/R_y \end{bmatrix}, \tag{12}$$

for real and nonnegative refractive indices. We adopt the usual sign convention for a radius, i.e., it is positive if the center of curvature is in the image space.

In taking the limit where R approaches zero, so $R_x \to R_y$, the torus becomes a sphere with radius $R_x = R_y \equiv R_{\text{sph}}$, the power matrix then reads

$$\mathbf{P}_{\text{spherical}} = -\frac{n' - n}{R_{\text{sph}}}\begin{bmatrix} 1 & 0 \\ 0 & 1 \end{bmatrix} \equiv -K\begin{bmatrix} 1 & 0 \\ 0 & 1 \end{bmatrix}, \tag{13}$$

with a refracting power K in units of dioptre or m^{-1}.

In the limit $R \to \infty$ the toroidal surface becomes cylindrical with radius $R_y \equiv R_{\text{cyl}}$, and its axis is parallel to the x axis. So the power matrix now becomes

$$\mathbf{P}_{\text{cylindrical}} = -\frac{n' - n}{R_{\text{cyl}}}\begin{bmatrix} 0 & 0 \\ 0 & 1 \end{bmatrix} = -K\begin{bmatrix} 0 & 0 \\ 0 & 1 \end{bmatrix}. \tag{14}$$

For a cylindrical surface that is rotated over an angle γ as shown in Fig. 2 the optical power matrix is now easily found by applying a coordinate rotation to Eq. (14), yielding the same results as Arsenault[3] found for a cylindrical lens, noting that $K = 1/f$, f being the focal length.

B. Derivation of the 4 × 4 Translation Matrix

For a translation over a distance d through a uniform medium (see Fig. 2) the following holds:

$$\begin{aligned} \mathbf{r}' - \mathbf{r} &= d\left(\frac{[\mathbf{k} + \delta\mathbf{k}]_{\|}}{[\mathbf{k} + \delta\mathbf{k}]_z} - \frac{[\mathbf{k}]_{\|}}{[\mathbf{k}]_z}\right) \\ &= d\left(\frac{\boldsymbol{\mu} + \delta\boldsymbol{\mu}}{\sqrt{n^2 - (\boldsymbol{\mu} + \delta\boldsymbol{\mu})^2}} - \frac{\boldsymbol{\mu}}{\sqrt{n^2 - \boldsymbol{\mu}^2}}\right). \end{aligned} \tag{15}$$

This is the difference between the translation term of an arbitrary ray and of that of the chief ray. The lowest-order series expansion of Eq. (15) in $\delta\boldsymbol{\mu}$ yields

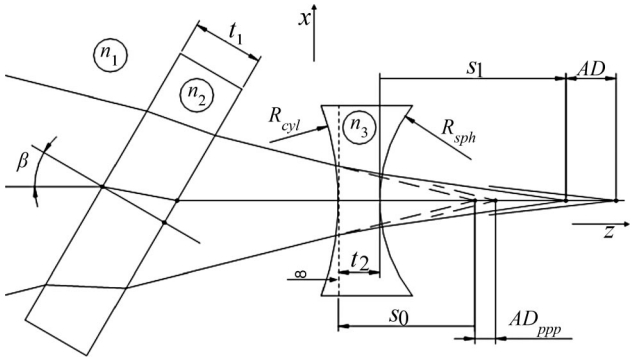

Fig. 3. Combination of a PPP with an anamorphic lens consisting of a cylindrical and a spherical surface. The orientation of the cylindrical axis is at an arbitrary angle γ with the x axis.

$$\begin{aligned} \mathbf{r}' - \mathbf{r} &= d\left(\frac{\delta\boldsymbol{\mu}}{\sqrt{n^2 - \boldsymbol{\mu}^2}} + \frac{(\boldsymbol{\mu}\cdot\delta\boldsymbol{\mu})\boldsymbol{\mu}}{(n^2 - \boldsymbol{\mu}^2)^{3/2}}\right) = \frac{d}{(n^2 - \boldsymbol{\mu}^2)^{3/2}} \\ &\times \begin{bmatrix} n^2 - \mu_y{}^2 & \mu_x\mu_y \\ \mu_x\mu_y & n^2 - \mu_x{}^2 \end{bmatrix}\begin{bmatrix} \delta\mu_x \\ \delta\mu_y \end{bmatrix} \equiv \mathbf{D}\delta\boldsymbol{\mu}, \end{aligned} \tag{16}$$

where $\mathbf{D}$ is the translation matrix. Using the partitioned matrices this becomes

$$\begin{bmatrix} \mathbf{r}' \\ \delta\boldsymbol{\mu}' \end{bmatrix} = \begin{bmatrix} \mathbf{1} & \mathbf{D} \\ \mathbf{0} & \mathbf{1} \end{bmatrix}\begin{bmatrix} \mathbf{r} \\ \delta\boldsymbol{\mu} \end{bmatrix} = [\mathbf{T}]\begin{bmatrix} \mathbf{r} \\ \delta\boldsymbol{\mu} \end{bmatrix}. \tag{17}$$

Again for paraxial rays the translation matrix reduces to the same result as was obtained by Arsenault:

$$\mathbf{D} = \frac{d}{n}\begin{pmatrix} 1 & 0 \\ 0 & 1 \end{pmatrix}. \tag{18}$$

The translation matrix can also be used to describe the properties of a PPP tilted over an angle β (see Fig. 3) around the y axis. For this we take the chief along $\boldsymbol{\mu} = (\sin\beta, 0)$ in the translation matrix after which the coordinate system is rotated such that the chief ray is along the optical axis. The direction vector for an arbitrary ray now becomes

$$n\delta\mathbf{k} = \left(\delta\mu_x,\ \delta\mu_y,\ \frac{-\boldsymbol{\mu}\cdot\delta\boldsymbol{\mu}}{\sqrt{1 - \boldsymbol{\mu}^2}}\right) = \left(\delta\mu_x,\ \delta\mu_y,\ \frac{-\mu_x\delta\mu_x}{\sqrt{1 - \mu_x{}^2}}\right). \tag{19}$$

Using the rotation matrix

$$\mathbf{R} = \begin{bmatrix} \cos\beta & 0 & -\sin\beta \\ 0 & 1 & 0 \\ \sin\beta & 0 & \cos\beta \end{bmatrix} = \begin{bmatrix} \sqrt{1 - \mu_x{}^2} & 0 & -\mu_x \\ 0 & 1 & 0 \\ \mu_x & 0 & \sqrt{1 - \mu_x{}^2} \end{bmatrix}, \tag{20}$$

we obtain

$$\mathbf{R}n\delta\mathbf{k} = \left(\frac{\delta\mu_x}{\sqrt{1 - \mu_x{}^2}},\ \delta\mu_y,\ 0\right). \tag{21}$$

Thus in the rotated coordinate system (ξ, y, ζ) the following holds:

$$\begin{bmatrix} (r'-r)_\xi \\ (r'-r)_\zeta \\ 0 \end{bmatrix} = \mathbf{R}\begin{bmatrix} D_{11} & D_{12} & 0 \\ D_{21} & D_{22} & 0 \\ 0 & 0 & 0 \end{bmatrix}\mathbf{R}^{-1}\begin{bmatrix} \delta\mu_\xi \\ \delta\mu_\zeta \\ 0 \end{bmatrix}, \quad (22)$$

which, after substituting Eq. (16) into Eq. (22), yields a new translation matrix:

$$\mathbf{D}' = \frac{d}{(n^2-\mu_x{}^2)^{3/2}}\begin{bmatrix} n^2(1-\mu_x{}^2) & 0 \\ 0 & n^2-\mu_x{}^2 \end{bmatrix} = \frac{d}{(n^2-\sin^2\beta)^{3/2}}\begin{bmatrix} n^2(1-\sin^2\beta) & 0 \\ 0 & n^2-\sin^2\beta \end{bmatrix}. \quad (23)$$

This can be rewritten as

$$\mathbf{D}' = \frac{d}{\sqrt{n^2-\sin^2\beta}}\begin{bmatrix} 1 & 0 \\ 0 & 1 \end{bmatrix} - \frac{d(n^2-1)\sin^2\beta}{(n^2-\sin^2\beta)^{3/2}}\begin{bmatrix} 1 & 0 \\ 0 & 0 \end{bmatrix}. \quad (24)$$

The factor in front of the anamorphic part of this matrix is the distance between the focal lines, also called astigmatic distance (AD), of a tilted PPP that relates to astigmatism in the following way[1]:

$$AD = \frac{(n^2-1)\sin^2\beta}{(n^2-\sin^2\beta)^{3/2}}\,d = \frac{2W_{22}}{NA^2}\,\lambda, \quad (25)$$

where W_{22} is the Seidel coefficient for astigmatism in units of wavelengths λ, and NA is the numerical aperture of the converging or diverging beam. The translation matrix for a tilted PPP is now defined as

$$\mathbf{D}_{\mathrm{ppp}} \equiv -AD\begin{bmatrix} 1 & 0 \\ 0 & 0 \end{bmatrix}. \quad (26)$$

Here we omitted the symmetric part of Eq. (24), which means that the lateral shift of the optical axis and the axial shift of the focal lines need to be taken into account separately. Intuitively, Eq. (26) can be regarded as an anamorpic translation from the first- to the second-focal line of the PPP. For a positive object distance going from the first- to the second-focal line the object distance becomes smaller, hence the minus sign in Eq. (26).

3. System Matrix

Here the theory from Section 2 is used to describe a system that contains a PPP and a lens with a spherical and a cylindrical surface. It will be shown how one can obtain closed expressions for the position and orientation of both focal lines and the location of the smallest spot.

The system under consideration here consists of a PPP having a refractive index of n_2 rotated around the y axis over an angle β followed by an astigmatic lens, (see Fig. 3). This astigmatic lens consists of a first surface that is cylindrical having a radius R_{cyl} and a second spherical surface with radius R_{sph}. The lens material has a refractive index n_3. The beam toward the PPP is converging toward the virtual source point at s_0 measured from the entrance surface of the astigmatic lens. The image distance is given by s_1 measured from the exit surface of this lens.

Using the matrix formalism of the preceding paragraph the system is written as

$$\begin{bmatrix} \mathbf{r}' \\ \delta\boldsymbol{\mu}' \end{bmatrix} = [\mathbf{T}(s_1)][\mathbf{L}_{\mathrm{sph}}]\left[\mathbf{T}\left(\frac{t_2}{n_3}\right)\right][\mathbf{R}(\gamma)][\mathbf{L}_{\mathrm{cyl}}][\mathbf{R}(\gamma)]^{-1} \times [\mathbf{T}(s_0)][\mathbf{T}_{\mathrm{ppp}}]\begin{bmatrix} \mathbf{r} \\ \delta\boldsymbol{\mu} \end{bmatrix} \equiv \mathbf{M}\begin{bmatrix} \mathbf{r} \\ \delta\boldsymbol{\mu} \end{bmatrix} \equiv \begin{bmatrix} \mathbf{I} & \mathbf{J} \\ \mathbf{K} & \mathbf{L} \end{bmatrix}\begin{bmatrix} \mathbf{r} \\ \delta\boldsymbol{\mu} \end{bmatrix}. \quad (27)$$

Here, $\mathbf{L}_{\mathrm{sph}}$, $\mathbf{L}_{\mathrm{cyl}}$, $\mathbf{T}$, and $\mathbf{R}$ are 4×4 matrices representing power, translation, and rotation operations, respectively. From this system matrix several imaging properties can be derived. For instance, from $\mathbf{I}$ and $\mathbf{L}$ the lateral and angular magnifications can be obtained, and $\mathbf{K}$ gives the power of the system. In this paper we will focus only on the information we can obtain from $\mathbf{J}$.

A. Imaging Condition

The coordinates of the image point are given by $\mathbf{r}' = \mathbf{I}\cdot\mathbf{r} + \mathbf{J}\cdot\delta\boldsymbol{\mu}$. When imaging using a rotation symmetrical lens system all rays leaving a point designated by $\mathbf{r}$ should arrive at the point given by $\mathbf{r}'$. This means that $\mathbf{r}'$ is independent of $\delta\boldsymbol{\mu}$ so $\mathbf{J} = \mathbf{0}$ is the imaging condition for a rotationally symmetric system. By solving $\mathbf{J} = \mathbf{0}$ one then finds the image distance. For an anamorphic system, such as we have here, this no longer holds. Instead of a focal point two focal lines can be found. The location of these focal lines can be found by solving $\mathbf{J}\cdot\delta\boldsymbol{\mu} = \mathbf{0}$. This is a characteristic equation of $\mathbf{J}$, which has nontrivial solutions only if $|\mathbf{J}| = \mathbf{0}$, which is our new imaging condition. Solving $|\mathbf{J}| = \mathbf{0}$ leads to a quadratic equation in s_1 yielding two solutions, i.e., the z position of both focal lines, and the difference between them yields the astigmatic distance of the system

$$0 = a's_1{}^2 + b's_1 + c',$$

$$s_1 = -\frac{b'}{2a'} \mp \sqrt{\left(\frac{b'}{2a'}\right)^2 - \frac{c'}{a'}},$$

$$AD_{\mathrm{syst}} = 2\sqrt{\left(\frac{b'}{2a'}\right)^2 - \frac{c'}{a'}}. \quad (28)$$

The coefficients of the quadratic equation can be expressed in the system design parameters, but as these

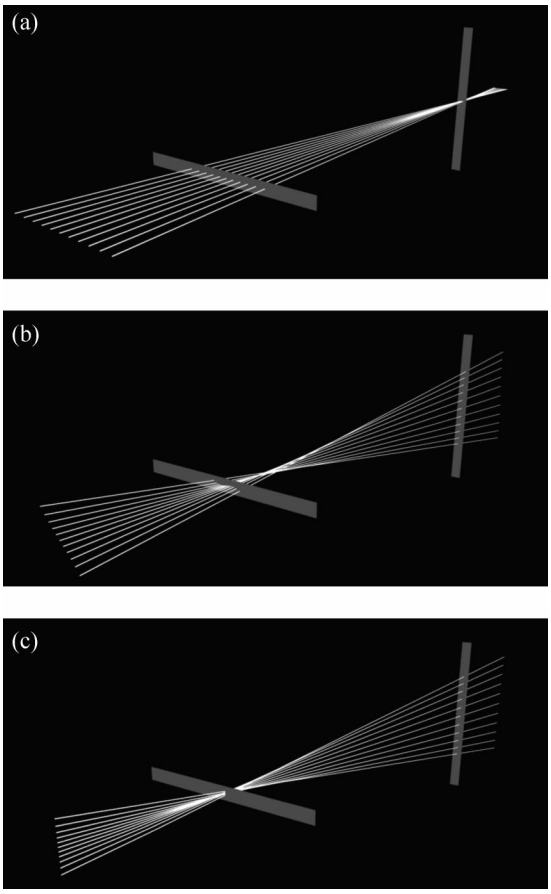

Fig. 4. Ray fans of a converging astigmatic beam with its first focal line in the x direction and hence the second focal line in the y direction. The first and second focal lines are indicated by the near and far gray rectangles, respectively. (a) A ray fan lying in the xz plane converges to a single focus at the second focal line. The ray fan shown in (c) is lying in the yz-plane and its rays come to focus at the first focal line. For a ray fan outside the xz and yz planes, as in (b), the rays do not come to a focus. This fan however rotates such that all its rays pass through both focal lines. Arsenault has described this rotation of ray fans earlier (Ref. 2).

expressions become rather lengthy we will present them in Appendix A. Together with the optical axis, each of the two (nontrivial) eigenvectors of $\mathbf{J}$ spans a plane in the object space. For these planes it holds that all rays lying in such a plane and leaving from the object point come together in one image point. This is illustrated by considering a converging astigmatic beam as shown in Fig. 4.

B. Focal Line Orientation

In $\mathbf{r}' = \mathbf{I} \cdot \mathbf{r} + \mathbf{J} \cdot \delta\boldsymbol{\mu}$ we substitute polar coordinates (ρ, ϕ) for the Cartesian coordinates $(\delta\mu_x, \delta\mu_y)$:

$$\begin{pmatrix} x' \\ y' \end{pmatrix} = \mathbf{I} \cdot \mathbf{r} + \mathbf{J} \begin{pmatrix} \rho \cos \phi \\ \rho \sin \phi \end{pmatrix} = \mathbf{I} \cdot \mathbf{r} + \rho \begin{pmatrix} J_{11} \cos \phi + J_{12} \sin \phi \\ J_{21} \cos \phi + J_{22} \sin \phi \end{pmatrix}. \quad (29)$$

By choosing a fixed value for ρ, Eq. (29) is a parametric equation in ϕ describing an ellipse in image space. In object space the rays fan out in a circular manner. The general parametric equation in t of an ellipse centered at $\mathbf{I} \cdot \mathbf{r}$ with major and minor semiaxes a and b with an angle φ between the x' axis and the major semiaxis is

$$\begin{pmatrix} x' \\ y' \end{pmatrix} = \mathbf{I} \cdot \mathbf{r} + \begin{pmatrix} a \cos \varphi \cos(t - \Delta) - b \sin \varphi \sin(t - \Delta) \\ a \sin \varphi \cos(t - \Delta) + b \cos \varphi \sin(t - \Delta) \end{pmatrix}, \quad (30)$$

where Δ is used for defining the starting point of the ellipse. From Eqs. (29) and (30), eliminating the respective parameters ϕ and t we get

$$\begin{cases} \rho \cdot J_{11} = a \cos \varphi \cdot \sin \Delta - b \sin \varphi \cdot \cos \Delta \\ \rho \cdot J_{12} = a \cos \varphi \cdot \cos \Delta + b \sin \varphi \cdot \sin \Delta \\ \rho \cdot J_{21} = a \sin \varphi \cdot \sin \Delta + b \cos \varphi \cdot \cos \Delta \\ \rho \cdot J_{22} = a \sin \varphi \cdot \cos \Delta - b \cos \varphi \cdot \sin \Delta. \end{cases} \quad (31)$$

From this result we can obtain the orientation of the first focal line by stating that $b = 0$ must hold, which yields

$$\tan \varphi = \frac{J_{21} + J_{22}}{J_{11} + J_{12}}. \quad (32)$$

By substituting the location of the first focal line, as given by Eq. (28), into Eq. (32) the angle between this focal line and the x' axis is found.

C. Spot of Least Confusion

We can also find the location of the spot of least confusion by using Eq. (31). Usually the spot of least confusion is considered to be a circle, and we have $a = b$.[1] However, more generally, the spot of least confusion turns out to be an ellipse whose location can be found by minimizing $(a - b)^2$:

$$(a - b)^2 = (J_{12} - J_{21})^2 + (J_{11} + J_{22})^2. \quad (33)$$

Working out Eq. (33) we find yet another quadratic equation in s_1 of which the extreme is given by

$$0 = a'' {s_1}^2 + b'' s_1 + c'',$$

$$s_1 = -\frac{b''}{2a''}. \quad (34)$$

Here also the coefficients of the quadratic equation can be expressed in the system design parameters. Equation (33) shows that $a = b$ if $J_{11} = -J_{22}$ and $J_{12} = J_{22}$. In this case the matrix $\mathbf{J}$ describes mirroring in a line. This means that the spot of least confusion is a circle only if the system is reflection symmetric in a plane containing both this line and the z axis, i.e., all the astigmatic elements have their symmetry axes lined up with or perpendicular to this

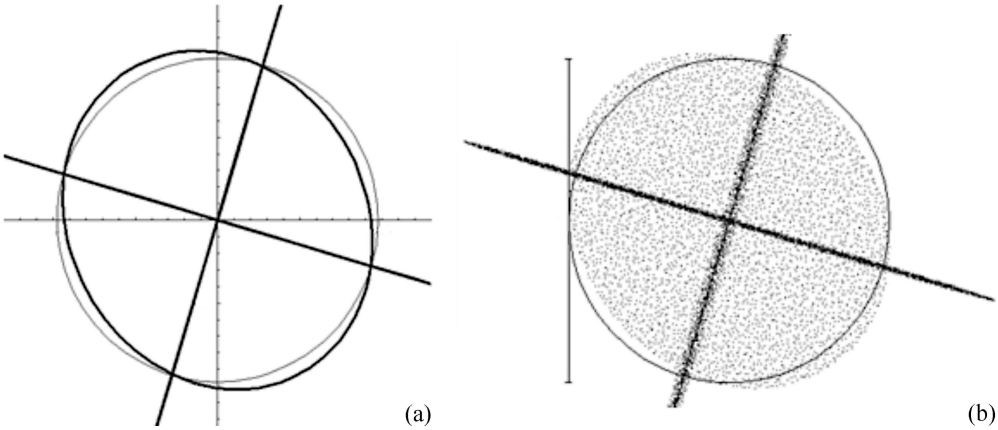

Fig. 5. Comparison between calculated (a) and simulated (b) results for the system shown in Fig. 3. The thin circles have the same area as the calculated spot of least confusion.

plane. The spot size is calculated by taking the diameter of the circle that has the same area as the ellipse at the spot of least confusion position:

$$\Phi = 2\sqrt{ab} = 2\rho\sqrt{J_{12}J_{21} - J_{11}J_{22}}. \tag{35}$$

Here ρ is equal to the numerical aperture NA of the beam incident in object space.

4. Comparison with Simulations and Measurements

In this section a comparison is made between the calculated results using the theory described above and the simulation results obtained using a ray-tracing program.[6] Furthermore, we compare experimental results with the calculated results.

A. Simulation Results

Using the system presented in Section 3, a design was made and the calculated results were compared to the ray-trace results. The design has the following parameters: $n_1 = 1.0$, $n_2 = 1.520241$, $n_3 = 1.579827$, $\beta = 45°$, $t_1 = 4.0$ mm, $t_2 = 0.9$ mm, $R_{cyl} = -12.0$ mm, $R_{sph} = 5.8$ mm, $s_0 = -3.3$ mm, NA = 0.0874, and $\gamma = 45°$.

The calculations yield for the positions of the first and second focal lines and the spot of least confusion $s_1 = 4.13693$, 8.18252, and 5.76945 mm, respectively. The first focal line makes an angle of $-16.5°$ with the horizontal x axis. The size of the spot of least confusion equals 195.3 μm. These parameters were used as input to the ray-trace calculation in which the PPP was split into two plates of half the thickness of the

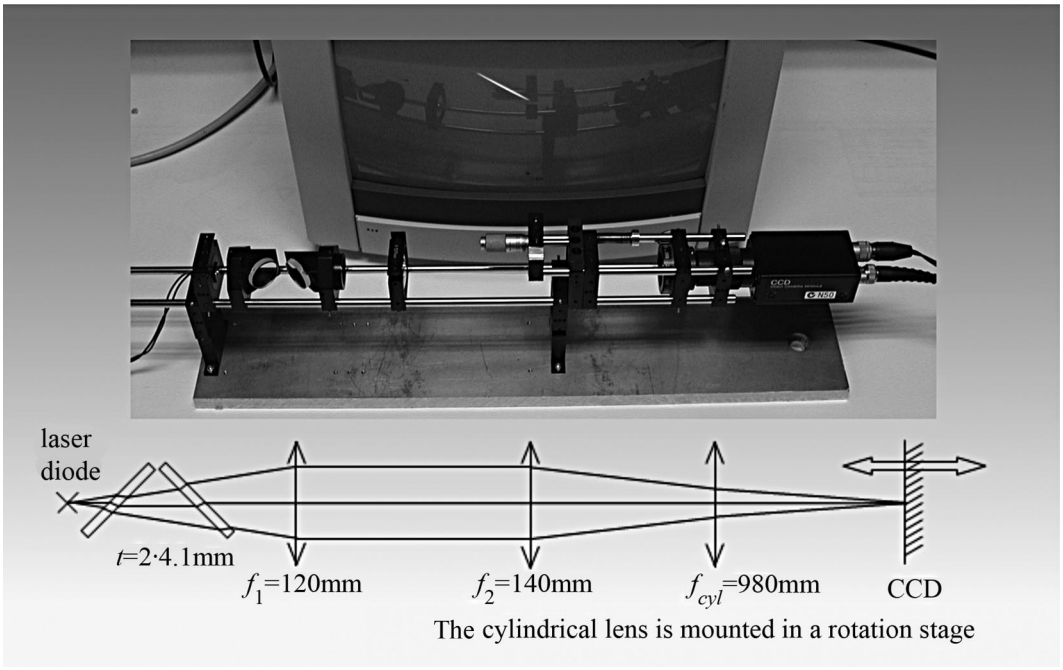

Fig. 6. Photo and outline of the experimental setup.

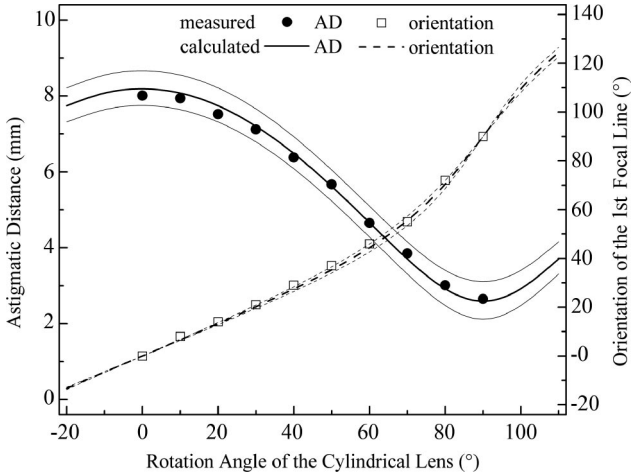

Fig. 7. Comparison between measured and calculated results.

single PPP. These were tilted in opposite directions around the same axis as is done in the measurement setup shown in Fig. 6 below. By doing so the astigmatism is the same as for the single PPP, but the coma is canceled. This also cancels the lateral shift of the optical axis. The axial shift of the focal lines, however, needs to be taken into account in the ray-trace model, so it is.

In Fig. 5(a) the calculated focal line is shown, and the simulated focal line and spot of least confusion are shown in Fig. 5(b). For comparison, a circle is drawn at the calculated spot size of 194.1 μm that shows that the spot of least confusion is indeed elliptical. The simulated results from the ray-trace program compare excellently to the calculated results.

B. Experimental Results

In Fig. 6 an experimental setup is shown in which a laser beam diverges as it passes through two 45° tilted PPPs. A lens with a focal length of $f_1 = 120$ mm is used to collimate the astigmatic beam emerging from the PPPs. A second lens, with $f_2 = 140$ mm, converges the collimated beam to a point somewhere behind the cylindrical lens, $f_{cyl} = 980$ mm, which is mounted in a rotation stage. A CCD camera on a translation stage is used to find and measure the positions and orientation of the focal lines for different rotation angles of the cylindrical lens.

The measured and calculated results are shown in Fig. 7. For the calculations all parameters were obtained from direct independent measurements. The thin curves in Fig. 7 give the calculation results for a 10% deviation in f_{cyl}. This shows that the astigmatic distance is relatively sensitive while the orientation of the first focal line, γ_{1st}, is rather insensitive to this change. The measurement errors are of the order of 0.02 mm for the astigmatic distance and 2° for γ_{1st}. Despite the small sensitivity of γ_{1st} to the change in f_{cyl} we can state that the measured and the calculated results are in excellent agreement due to the small measurement errors and because the calculated line for γ_{1st} predicts the measurements very well. In the absence of the PPPs the latter line would be straight going through the origin with a slope of 1.0.

5. Summary and Conclusions

A paraxial model was derived for the plane-parallel plate using the 4×4 matrix formalism of Arsenault. The model has been used to build a system description of a plane-parallel plate combined with a servo lens. From the system matrix several imaging properties were derived. These were used to analyze a particular system whose results were compared to the ray-tracing results. The same was done for the experimental results. In both cases excellent agreement was obtained.

One particular outcome of the system description is that in general not a circle but an ellipse of least confusion is found when two sources of astigmatism are combined. The model derived here for a plane-parallel plate, combined with the already existing models for the lens surfaces, enabled us to design a system comprising such a plane-parallel plate.

Appendix A. Elaboration of the System Matrix

In this appendix we elaborate the system matrix $\mathbf{M}$ to obtain its 2×2 matrix element $\mathbf{J}$ that in turn will be elaborated to find the coefficients for the quadratic Eqs. (28) and (34). Working out the system matrix (27) we find for $\mathbf{J}$

$$\begin{aligned}\mathbf{J} = \{\mathbf{D}(s_1)\cdot\mathbf{P}_{sph} + \mathbf{1}\}\cdot\Bigg\{\mathbf{D}\left(s_0 + \frac{t_2}{n_3} - AD_{ppp}\right) \\ + \mathbf{D}\left(\frac{t_2}{n_3}\right)\cdot\mathbf{R}(\gamma)\cdot\mathbf{P}_{cyl}\cdot\mathbf{R}^{-1}(\gamma)\cdot\mathbf{D}(s_0 - AD_{ppp})\Bigg\} \\ + \mathbf{D}(s_1)\{\mathbf{R}(\gamma)\mathbf{P}_{cyl}\mathbf{R}^{-1}(\gamma)\mathbf{D}(s_0 - AD_{ppp}) + \mathbf{1}\}.\end{aligned} \tag{A1}$$

Here we have used a shorthand notation for the sum of translation matrices, e.g., $\mathbf{D}(s_0) + \mathbf{D}_{ppp}$ is written as $\mathbf{D}(s_0 - AD_{ppp})$. Extending (A1) yields

$$\begin{cases} J_{11} = s_1 + (1 - s_1K_{sph})(s_0 - AD_{ppp} + t_2/n_3) - [(1 - s_1K_{sph})t_2/n_3 + s_1](s_0 - AD)K_{cyl}\sin^2\gamma \\ J_{12} = [s_1(1 - K_{sph}t_2/n_3) + t_2/n_3]s_0K_{cyl}\sin\gamma\cos\gamma \\ J_{21} = [s_1(1 - K_{sph}t_2/n_3) + t_2/n_3](s_0 - AD_{ppp})K_{cyl}\sin\gamma\cos\gamma \\ J_{22} = s_1 + (1 - s_1K_{sph})(s_0 + t_2/n_3) - [(1 - s_1K_{sph})t_2/n_3 + s_1]s_0K_{cyl}\cos^2\gamma. \end{cases} \tag{A2}$$

Substituting (A2) into $|\mathbf{J}| = (J_{11}J_{22}) - (J_{12}J_{21})$ gives

$$
\begin{aligned}
a' &= 1 + K_{\mathrm{sph}}{}^2(s_0 + t_2/n_3)(s_0 + t_2/n_3 - AD_{\mathrm{ppp}}) \\
&\quad - K_{\mathrm{sph}}[2(s_0 + t_2/n_3) - AD_{\mathrm{ppp}}] - K_{\mathrm{sph}}K_{\mathrm{cyl}}(K_{\mathrm{sph}}t_2/n_3 \\
&\quad - 1)\big(s_0(s_0 + t_2/n_3 - AD_{\mathrm{ppp}}) - AD(t_2/n_3)\sin^2\gamma\big) \\
&\quad + K_{\mathrm{cyl}}(K_{\mathrm{sph}}t_2/n_3 - 1)\big(s_0 - AD_{\mathrm{ppp}}\sin^2\gamma\big), \\
b' &= 2(s_0 + t_2/n_3) - AD_{\mathrm{ppp}} - 2K_{\mathrm{sph}}(s_0 + t_2/n_3) \\
&\quad \times (s_0 + t_2/n_3 - AD_{\mathrm{ppp}}) + K_{\mathrm{cyl}}(2K_{\mathrm{sph}}t_2/n_3 - 1) \\
&\quad \times \big[s_0(s_0 + t_2/n_3 - AD_{\mathrm{ppp}}) - AD_{\mathrm{ppp}}(t_2/n_3)\sin^2\gamma\big] \\
&\quad - K_{\mathrm{cyl}}(t_2/n_3)\big(s_0 - AD_{\mathrm{ppp}}\sin^2\gamma\big), \\
c' &= (s_0 + t_2/n_3)(s_0 + t_2/n_3 - AD_{\mathrm{ppp}}) - K_{\mathrm{cyl}}(t_2/n_3)\big[s_0(s_0 \\
&\quad + t_2/n_3 - AD_{\mathrm{ppp}}) - AD_{\mathrm{ppp}}(t_2/n_3)\sin^2\gamma\big], \qquad \text{(A3)}
\end{aligned}
$$

which upon substitution into Eq. (28) yields the positions of the focal lines and the total AD of the system.

References

1. J. Braat, "Analytical expressions for the aberration coefficients of a tilted plane parallel plate," Appl. Opt. **36,** 8459–8466 (1997).
2. H. H. Arsenault, "The rotation of light fans by cylindrical lenses," Optics Commun. **31,** 275–278 (1979).
3. H. H. Arsenault, "A matrix representation for non-symmetrical optical systems," J. Opt. **11,** 87–91 (1980).
4. J. Schleipen, B. Hendriks, and S. Stallinga, "Optical heads," in *Encyclopedia of Optical Engineering* (Marcel Dekker, 2003), pp. 1666–1693.
5. Eric W. Weisstein, "Torus," from MathWorld-A Wolfram Web Resource, http://mathworld.wolfram.com/Torus.html.
6. The ray-trace program used ZEMAX, www.zemax.com.